

Decoherence and Quantum Freeze through Stroboscopic Measurements and Injections: The Environment as a Measurement Apparatus.

Gonzalo A. Álvarez, Ernesto P. Danieli, Patricia R. Levstein, and Horacio M. Pastawski
Facultad de Matemática, Astronomía y Física, Universidad Nacional de Córdoba, Ciudad Universitaria, 5000, Córdoba, Argentina

Cross-polarization NMR data, swept over a wide range of system-environment interaction strengths, are interpreted by solving the swapping dynamics between two coupled spins (qubits) interacting with a spin bath. We introduce a model where the interaction with the real environment is represented as a stroboscopic process. This instantaneous interaction interrupts the system evolution through measurements and/or injections. This picture, that is extended to a continuous process, leads to an efficient algorithm where decoherence and dissipation mechanisms emerge naturally. From the theoretical and experimental results we characterize two dynamical phases, essential for quantum information processing: a swapping phase and a Zeno phase.

PACS numbers: 03.65.Yz, 03.65.Ta, 03.65.Xp, 76.60.-k

The control of coherent dynamics in quantum systems has a fundamental relevance in Quantum Information Processing (QIP) [1]. Experiments on QIP involve atoms in optical traps [2], superconducting boxes [3] and nuclear spins [4, 5] among others. Typically, the system to be manipulated interacts with an environment [2, 6, 7, 8] that smoothly degrades its quantum dynamics. Moreover, this “decoherence” can be controlled by the own system’s complexity [9]. Thus, a precise understanding of its inner mechanisms is critical. This is the case of the control of the swapping gate, an essential building block for QIP. While the swapping operation was recently addressed in the field of liquid NMR [10, 11], pioneer experiments under well controlled conditions were done in solid state NMR [12] by Müller, Kumar, Baumann and Ernst (MKBE). They characterized a swapping frequency depending on the system parameters and a relaxation rate, depending only on interactions with the bath, where decoherence and dissipation were not explicitly distinguished. The dynamics was obtained by solving a generalized Liouville-von Neumann equation where the degrees of freedom of the environment, typically a boson bath, are traced out to yield a Quantum Master Equation (QME) [13]. However, more recent experiments, controlling the ratio between internal and system-environment interactions (SEI) [14], show an abrupt change in the behavior of the swapping frequency and relaxation rates not predicted by MKBE. These striking results can not be explained within the standard approximations in the QME.

In this letter, we present an alternative dynamical model that allows one to understand the experiments and sheds new light on the processes involved in any swapping operation. In our model the interaction between a system of two coupled spins and a real environment, a spin bath, is represented as a stroboscopic process that interrupts the system evolution with *certain probability*. This picture emerges from the quantum theory of irreversible processes expressed in the Keldysh formalism [15]. This stroboscopic process measures and/or injects polarization density

depending on the SEI and the bath state. The joint limit of continuous interruption and infinitesimal probability enables one, not only to recover time scales consistent with a Fermi Golden Rule description, but more importantly, to distinguish the parts of the interaction that lead to dissipation from those giving pure decoherence. Within this description, it is clear that a change in the ratio between internal and SEI enables a switch from *swapping* (sub-damped) to *Zeno* (over-damped) dynamical phases. In the last case, the environment “measures” the system very frequently, giving rise to the quantum Zeno effect (QZE) [16, 17]. The switch between these phases accounts for the singular experimental behavior observed in ref. [14].

Consider M coupled $1=2$ spins with a Hamiltonian:

$$H = H_z + \sum_{i < j} \left(a_{ij} I_i^z I_j^z + \frac{1}{2} b_{ij} (I_i^+ I_j + I_i I_j^+) \right) ; \quad (1)$$

where $H_z = \sum_{i=1}^M \omega_i I_i^z$ is the Zeeman energy, with a mean frequency ω_0 . The second term gives the spin-spin interaction: $b_{ij}=a_{ij}=0$ is Ising, and $a_{ij}=b_{ij}=0; 1; 2$ gives an $X Y$, an isotropic (Heisenberg) or the truncated dipolar (secular) Hamiltonian, respectively. This last case is typical in solid-state NMR experiments [13] where $\omega_i; a_{ij}; b_{ij} \sim \omega_0$.

Spin-Fermion mapping.— In order to describe the experimental system [12, 14], let us take the first $N = 2$ spins, I_1 (a ^{13}C) and I_2 (its directly bonded ^1H), as the “system”. The other $M - N$ spins (all the other ^1H), with $M - 1$, are the “spin bath”. The spin system can be mapped into a fermion particle system using the Jordan-Wigner Transformation (JWT) [18], $I_i^+ = c_i^+ \exp i \sum_{j=1}^{i-1} c_j^+ c_j$. Under the experimental conditions, $\omega_i = 0; a_{12} = 0$ and $b_{12} = b$; the system Hamiltonian becomes:

$$H_s = \omega_0 c_1^+ c_1 + c_2^+ c_2 \left(1 + \frac{b}{2} c_1^+ c_2 + c_2^+ c_1 \right) ; \quad (2)$$

The JWT maps a linear many-body $X Y$ spin Hamiltonian into a system of non-interacting fermions. This leads us to solve a one-body problem, reducing the dimension of

the Hilbert space from 2^N to N states that represent local excitations [18]. To simplify the presentation, and without loss of generality, we consider a *single* connection between the system and the spin bath, $a_{23} = d_{23}$ and $b_{23} = d_{23}$ with $a_{2j} = b_{2j} = 0$; $j = 4::1$ and $a_{1j} = b_{1j} = 0$; $j = 3::1$. Spins I_1 with 3 i M are interacting among them. The SEI becomes:

$$V = d_{23} \left(c_2^\dagger c_2 - \frac{1}{2} \right) \left(c_3^\dagger c_3 - \frac{1}{2} \right) + \frac{1}{2} \left(c_2^\dagger c_3 + c_3^\dagger c_2 \right) \quad (3)$$

In the first (Ising) term, the first factor “measures” if there is a particle at site 2 while the second “measures” at site 3. Hence, polarization at site 2 becomes the observable detected by the environment. The hopping term swaps particles between bath and system.

Stroboscopic Decoherent Model.— In the experimental initial condition, all spins are polarized with the exception of I_1 [12, 19]. In the high temperature limit ($\sim \beta_0 = k_B T$ s 1), the reduced density operator ($\rho(0) = \tilde{G}^<(0) = (1 + sI_2^z) = \text{Tr} \rho_{\text{flg}}$ which under the JWT becomes $\frac{(1 - s=2)}{\text{Tr} \rho_{\text{flg}}} 1 + \frac{s}{\text{Tr} \rho_{\text{flg}}} c_2^\dagger c_2$: Since the first term does not contribute to the dynamics, we retain only the second term and normalize it to the occupation factor. This means that site 1 is empty while site 2 and sites at the particle reservoir are “full”. This describes a tiny mean occupation excess above $1=2$ whose dynamical fluctuations are essential to produce decoherence in the system. To solve the reduced density matrix of the “system” $G^<(t) = \tilde{G}^<(t)$; we will take advantage of the particle representation and use an *integral* form [15] of the Keldysh formalism instead of the standard Liouville-von Neumann differential equation. There, any perturbation term is accounted to infinite order ensuring the proper density norm. The interaction with the bath is *local* and, because of the fast bath dynamics, it can be taken as *instantaneous*. Hence, the evolution is further simplified into an integral form of the Generalized Landauer Büttiker Equation (GLBE) [20] for the particle density. There, the environment plays the role of a local measurement apparatus. Firstly, we discuss the physics in this GLBE by developing a discrete time version where the measurements occur at a *stroboscopic time* τ_s .

We introduce our stroboscopic decoherent model operationally for an Ising form for V ($= = 0$). The initial state of the isolated two-spin system evolves with H_s . At τ_s , the spin bath interacts instantaneously with the “system” interrupting it with a probability p . Considering that the dynamics of the bath is much faster than that of the system (fast fluctuation approximation), the dynamics of site 3 produces an energy fluctuation on site 2 that destroys the coherence of the two-spin “system”. This represents the “measurement” process that collapses the “system” state. At time τ_s , the “system” evolution splits into three alternatives: with probability $1 - p$ the state survives the interruption and evolves unaffectedly, while with probability p the system is effectively interrupted and its evolution starts again from each of the *two* eigenstates of $c_2^\dagger c_2$. These three

possible states at τ_s evolve freely until the system is monitored again at time $2\tau_s$ and a new branching of alternatives is produced as in the scheme in Fig. 1(a).

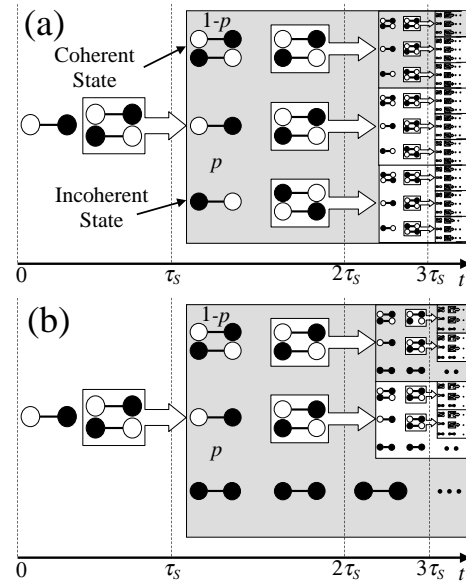


FIG. 1: Stroboscopic decoherent sequence for (a) an Ising interaction and (b) an isotropic one. Single states represent interrupted states (incoherent) and pairs of states are coherent superpositions. Notice the self-similar structure.

A similar reasoning holds when $\epsilon \neq 0$: The sequence for isotropic interaction ($= =$) is shown in Fig. 1(b). The $X Y$ part of V can inject a particle. When an interruption occurs, the bath “measures” at site 2 and, if found empty, it injects a particle. In the figure, this can be interpreted as a “pruning” of some incoherent branches increasing the global coherence. This explains why the rate of *decoherence is greater when the Ising part of V dominates over the $X Y$ part*. This occurs with the dipolar interaction and, in less degree, with the isotropic one. This contrasts with a pure $X Y$ interaction where the survival of spin coherences is manifested by a “spin wave” behavior [21]. The empty site of the bath is refilled and de-correlates in a time much shorter than the swapping between sites 1 and 2 (fast fluctuation approximation). Consequently, the injection can only occur from the bath toward the system.

Analytic description.— The evolution between interruptions is governed by the system’s propagators $G^{\text{OR}}(t) = \frac{1}{\tilde{z}} \exp[-iH_s t]$ and $G^{\text{OA}}(t) = G^{\text{OR}}(t)^Y$. The spin bath interacts with the system stroboscopically through an instantaneous *interruption function* $e^<(t) = \frac{1 - s}{\tilde{z} p} c^<(t)$. The reduced density function is

$$\frac{1}{\tilde{z}} G^<(t) = G^{\text{OR}}(t) G^<(0) G^{\text{OA}}(t) (1 - p)^n + \sum_{m=1}^n G^{\text{OR}}(t - t_m) e^<(t_m) G^{\text{OA}}(t - t_m) p (1 - p)^{n-m}; \quad (4)$$

where $n = \text{int}(t/\tau_s)$ is the number of interruptions and $t_m = m\tau_s$. The first term in the rhs is the coherent system evolution weighted by its survival probability $(1-p)^n$: This is the upper branch in Fig. 1. The second term is the incoherent evolution involving all the decoherent branches. The m -th term in the sum represents the evolution that had its last interruption at $m\tau_s$ and survived coherently from $m\tau_s$ to $n\tau_s$. Each of these is composed by all the interrupted branches in Fig. 1 with a single state at the hierarchy level m with whom the paired state in the upper branch, generated at time $(m+1)\tau_s$; keeps coherence up to $n\tau_s$. We rearrange expression (4), for $n\tau_s < t < (n+1)\tau_s$; in terms of $n\tau_s$; the last interruption time:

$$\frac{1}{\tau_s} G^<(t) = G^{OR}(t - t_n) G^<(t_n) G^{OA}(t - t_n) (1-p)^n + G^{OR}(t - t_n) e^<(t_n) G^{OA}(t - t_n); \quad (5)$$

which takes advantage of the self similarity of the hierarchy levels and is very simple to iterate.

Continuous process.— In the limits $p \rightarrow 0$ and $\tau_s \rightarrow 0$ with constant ratio, one gets a continuous process where $\tau_s = \tau_s/p$ defines a survival time for the evolution of the isolated two-spin “system”. Eq. (4) becomes

$$\frac{d}{dt} G^<(t) = -\tau_s^{-1} G^{OR}(t) G^<(0) G^{OA}(t) e^{-t/\tau_s} + \dots \quad (6)$$

a new form of the GLBE [20] that includes correlations (non-diagonal terms in $G^<$ and $G^<$). Moreover, keeping τ_s constant, under the conditions of finite τ_s . $\tau_s \approx d_{23}$ and $p \approx d_{23}/d_b$ (here d_b is a mean intra-bath interaction) there is no significant difference between the stroboscopic and the continuous descriptions. Thus, the physics of a quantum theory of irreversible processes [22] is obtained by adapting a collapse theory [23] into the probabilistic branching scheme represented in Fig. 1. The solutions of Eqs. (4) and (6) are both computationally demanding since they involve a storage of all the previous time steps and reiterated summations. However, Eq. (5) provides a *new computational procedure* that only requires the information of a *single* previous step. Besides, it avoids random averages required in models that include decoherence through stochastic or kicked-like perturbations [24]. Thus, it becomes a very practical tool to compute the dynamics in presence of decoherent and dissipation processes.

The above procedure gives a novel physical meaning for the Keldysh’s self-energy [20] as an *instantaneous interruption function*: $G^<(t) = G^<(t) + G_d^<(t)$. Dissipation processes are in $G_d^<(t)$ while $G^<(t)$ involves only decoherence. In matrix form,

$$\frac{d}{dt} \begin{pmatrix} G^<(t) \\ G_d^<(t) \end{pmatrix} = \begin{pmatrix} -\tau_s^{-1} G^{OR}(t) & 0 \\ 0 & -\tau_s^{-1} G^{OA}(t) \end{pmatrix} \begin{pmatrix} G^<(t) \\ G_d^<(t) \end{pmatrix} + \begin{pmatrix} 0 \\ \tau_s^{-1} G^{OA}(t) \end{pmatrix}; \quad (7)$$

$$\frac{d}{dt} \begin{pmatrix} G^<(t) \\ G_d^<(t) \end{pmatrix} = 2i \begin{pmatrix} -\tau_s^{-1} p_{XY} & 0 \\ 0 & 1 \end{pmatrix} \begin{pmatrix} G^<(t) \\ G_d^<(t) \end{pmatrix}; \quad (8)$$

The term $G_d^<(t)$ injects a particle, increasing the system density, provided that site 2 is empty. This occurs at an *injection rate* $p_{XY} = \tau_s^{-1} p_{XY}$ with $p_{XY} = [2\tau_s^{-1} (d^2 + d^2)]$; the $X Y$ interaction weight. The decoherent part, $G^<(t)$; is a consequence of the “measurement” (or *interruption*) performed by the environment. It collapses the state vanishing the non-diagonal terms (coherences) with a *measurement rate* $\tau_s^{-1} p_{XY} = (1 - p_{XY}) \tau_s^{-1}$: This also occurs with the $X Y$ interaction with rate $p_{XY} \tau_s^{-1}$ regardless of the fact that an effective injection takes place. Then, the inverse of the survival time or *interruption rate* is $\tau_s^{-1} = \tau_s^{-1} p_{XY} + \tau_s^{-1} (1 - p_{XY})$. Unlike $G_d^<(t)$, this process conserves the total polarization. If τ_s^{-1} is the isotropic rate ($d^2 = d^2 = 1$), we have for the anisotropic case: $\tau_s^{-1} = \tau_s^{-1} (d^2 + d^2)$; then $\tau_s^{-1} = \tau_s^{-1} (d^2 + d^2)$. When the bath is a chain of spins with $X Y$ interactions [25], $\tau_s^{-1} = 2 d_{23}^2 (d_b)^{-1}$; in agreement with the Fermi Golden Rule.

The anisotropy ratio (d^2/d^2) accounts for the observed competition [19] between the Ising and $X Y$ terms of V . The Ising interaction leads the “system” to a quasiequilibrium state given by its Boltzmann distribution: In contrast, the $X Y$ term allows the thermal equilibration with the bath [19]. Inserting Eq. (7) into Eq. (6) that we solve to obtain our main analytical result:

$$\tau_s^{-1} G_{11}^<(t) = 1 - a_0 e^{R_0 t} - a_1 \cos(\omega t + \phi_0) e^{R_1 t}; \quad (9)$$

where ω ; R_0 and R_1 as well as a_0 , a_1 and ϕ_0 depend only on b ; τ_s and p_{XY} . In the appendix we show a complete analytical expression.

Limiting cases: Stroboscopic Model vs. QME.— Typical solutions of the QME [13] for a spin swapping [19] follow that of MKBE [12]. They considered an *isotropic interaction* with the spin environment, represented by a phenomenological relaxation rate $R = \tau_s^{-1} p_{XY}$: Within the fast fluctuation approximation and neglecting non-secular terms, this leads to $\tau_s^{-1} G_{11}^{MKBE}(t) = 1 - \frac{1}{2} e^{R t} \frac{1}{2} e^{-\frac{1}{2} R t} \cos \frac{b}{2} t$; used in most of the experimental fittings. Our Eq. (9) reproduces this result under the condition $1=2 = \tau_s^{-1} p_{XY} = R = \tau_s^{-1} p_{XY}$ with an isotropic interaction Hamiltonian $V = V = 1$. However, at short times $t \ll \tau_s$; the MKBE swapping probability grows exponentially with a rate $1=2$. In contrast, our solution manifests the correct polarization growth in time, $\frac{1}{2} b \tau_s^{-2} t^2$; made possible by the initial phase ϕ_0 . Moreover, under the condition $b \approx \tau_s^{-1}$, this enables the manifestation of the QZE [2, 16, 17]. This means that the bath frequently interrupts the system through measurements, freezing its evolution. At longer times, $t \gg \tau_s$, one gets $1 - \tau_s^{-1} G_{11}^<(t) \approx 1 + \frac{1}{2} b^2 \tau_s^{-2} \exp -\frac{1}{2} b^2 \tau_s^{-2} t$; and the QZE is manifested in the reduction of the decay rate $R = \frac{1}{2} b^2 \tau_s^{-2}$ as τ_s gets smaller than $\tau_s \approx b$. Another relevant result is that the frequency depends not only on b as in MKBE, but also on τ_s : A remarkable difference of the QME with our formulation concerns the final state. In the

QME it must be hinted beforehand, while here it is reached dynamically from the interaction with the spin bath. Here, the reduced density, whose trace gives the system polarization, can fluctuate until it reaches its equilibrium value.

Experimental switch among dynamical phases.— When the SEI is *anisotropic* ($\epsilon \neq 1$), there is a functional dependence of ω on b yielding frequencies in two dynamical regimes: 1- A *swapping phase*, which is a form of sub-damped parametric regime ($b < b_c$); 2- A *Zeno phase*, where an over-damped dynamics ($b > b_c$) appears as a consequence of the strong coupling with the environment (i.e. *imaginary frequency* in Eq. (9)). These dynamical regimes for *two* qubits enhance the results for a *single* qubit [6, 22] where a similar behavior was obtained by other approaches. The two dynamical phases can now be identified in NMR experiments on a molecular crystal, which up to date defied explanation. Experimental data taken from ref. [14] are shown in Fig. 2. There, the SEI is approximately constant ($\epsilon \approx 1$) while the system dynamics (b) is systematically modified through the orientation of a molecular axis (see ref. [14] for details). This provides a full scan of the parameter b through the phase transition that is manifested when the frequency goes suddenly to zero (Fig. 2(b)) and the relaxation rate (Fig. 2(a)) changes its behavior decaying abruptly. The fact that R tends to zero when $b \sim b_c$ evidences the QZE predicted by our model. In this regime, R is quadratic on b as predicted above. We verify that Eq. (9) reproduces the experimental swapping dynamics (Fig. 5 in ref. [14]) for each value of b , a constant ω and a dipolar V [26]. To make this comparison quantitative, we fit data generated with Eq. (9) with the same procedure used in ref. [14] obtaining the phenomenological relaxation rate R and the oscillation frequency ω (solid lines in Fig. 2).

This simple stroboscopic model enables a deep understanding of the processes involved in the SEI during an experimental realization of a swapping operation. The distinction of the processes that produce dissipation from those that only induce decoherence emerges naturally. Moreover, it provides an efficient algorithm which reduces numerical calculation times reproducing the results obtained from the quantum theory of continuous irreversible processes [20]. It is also remarkable that this model allows one to describe decoherence from two different perspectives: On one hand, as the survival time for the coherent (isolated) evolution of the system. This establishes a very pure concept of decoherence. On the other hand, as the more standard decay rate of the non-diagonal elements of the density matrix. They essentially coincide within the swapping regime. However, they differ in the Zeno phase. Here, the unaffected branch of evolution decays very fast with a rate $\sim 1/\tau$. In spite of this, for the swapping initial state one can see that the state as a whole does not decay (the dynamics is frozen) because of a feed by the environment. This is also reflected as the lack of decay of the non-diagonal terms of the density matrix in the H_S basis.

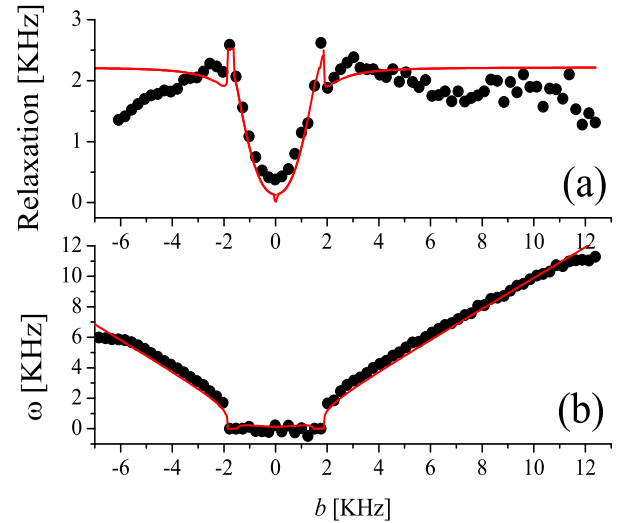


FIG. 2: (Color online) Relaxation rate R and frequency ω predicted by our model (solid lines) assuming a constant ϵ . The data points were obtained in ref. [14] after fitting cross polarization experiments to the expression $1 - \rho_{11} = 2 \exp(-Rt) \cos(\omega t) + 2 \exp(-2Rt)$: The parabolic behavior of R for $b \sim b_c$ corresponds to the overdamped Zeno phase.

Hence, through this understanding it is possible to interpret the overdamped experimental phase [14] as a simple realization of a decoherence-free subspace [17] obtained through the QZE.

We acknowledge support from Fundaci3n Antorchas, CONICET, FoNCyT, and SeCyT-UNC. This work was benefited from discussions with Lucio Frydman, who suggested experimental settings where these results are relevant, as well as stimulating comments from Alex Pines during a stay of PRL and HMP at the Weizmann Institute of Science.

APPENDIX

The main analytical result is Eq. (9),

$$\rho_{11}^< (t) = 1 - a_0 e^{-R_0 t} - a_1 \cos(\omega t + \phi_0) e^{-R_1 t};$$

with

$$R_0 = \frac{1}{2} \left[6 \frac{\langle P_{XY}; \mathbf{x} \rangle}{\langle P_{XY}; \mathbf{x} \rangle} + \frac{1}{6} (\langle P_{XY}; \mathbf{x} \rangle + \langle P_{XY}; \mathbf{x} \rangle + \frac{1}{3} (1 - \langle P_{XY}; \mathbf{x} \rangle)) \right];$$

$$R_1 = \frac{3}{4} \langle P_{XY}; \mathbf{x} \rangle + \frac{1}{3} (1 - \langle P_{XY}; \mathbf{x} \rangle) \frac{1}{6} R_0;$$

$$\omega = \frac{1}{4x} \frac{1}{6} (\langle P_{XY}; \mathbf{x} \rangle) + 6 \frac{\langle P_{XY}; \mathbf{x} \rangle}{\langle P_{XY}; \mathbf{x} \rangle} b;$$

and

$$a_0 = \frac{1}{8} \frac{8!^2 + 8R_1^2}{(R_0 + R_1)^2} b^2;$$

$$a_2 = \frac{1}{8!} \frac{(8R_0R_1 + b^2)(R_0 + R_1) + 8!^2 R_0}{(R_0 + R_1)^2};$$

$$a_3 = \frac{1}{8} \frac{b^2 + 8R_0^2}{(R_0 + R_1)^2} \frac{16R_0R_1}{(R_0 + R_1)^2};$$

$$a_1^2 = a_2^2 + a_3^2 \quad \tan(\theta) = \frac{a_2}{a_3};$$

where $x = b \sim$ and

$$P_{XY}(x) = \frac{1}{3} x^2 P_{XY}^2 + \frac{1}{3} (1 - P_{XY})^2;$$

$$P_{XY}(x) = \frac{1}{n} \left[4(1 - P_{XY})^2 9x^2 + 2(1 - P_{XY})^2 + 18P_{XY}^2 + 12 \cdot 3 \cdot 4x^6 (1 - P_{XY})^2 + 12P_{XY}^2 x^4 + 4P_{XY}^2 + 5(1 - P_{XY})^2 + 3P_{XY}^2 x^2 + 4P_{XY}^2 (1 - P_{XY})^2 P_{XY}^2 \right]^{\frac{1}{2}};$$

Electronic address: patricia@famaf.unc.edu.ar

- [1] C. H. Bennett and D.P. DiVincenzo, *Nature* **404**, 247 (2000).
 [2] C. J. Myatt *et al.*, *Nature* **403**, 269 (2000).
 [3] D. Vion *et al.*, *Science* **296**, 886 (2002).
 [4] M. Poggio *et al.*, *Phys. Rev. Lett.* **91**, 207602 (2003).

- [5] N. Boulant *et al.*, *Phys. Rev. A* **68**, 032305 (2003).
 [6] S. A. Gurvitz *et al.*, *Phys. Rev. Lett.* **91**, 066801 (2003).
 [7] W. H. Zurek, *Rev. Mod. Phys.* **75**, 715 (2003).
 [8] T. M. Stace and S.D. Barrett, *Phys. Rev. Lett.* **92**, 136802 (2004).
 [9] H.M. Pastawski *et al.*, *Physica A* **283**, 166 (2000).
 [10] Z.L. Mádi, R. Brüschweiler, R.R. Ernst, *J. Chem. Phys.* **109**, 10603 (1998).
 [11] N. Linden *et al.*, *Chem. Phys. Lett.* **307**, 198 (1999).
 [12] L. Müller *et al.*, *Phys. Rev. Lett.* **32**, 1402 (1974).
 [13] A. Abragam, *The Principles of Nuclear Magnetism* (Clarendon Press, Oxford, 1961).
 [14] P.R. Levstein, G. Usaj and H.M. Pastawski, *J. Chem. Phys.* **108**, 2718 (1998).
 [15] L.V. Keldysh, *ZhETF* **47**, 1515 (1964) [*Sov. Phys.-JETP* **20**, 335 (1965)]; P. Danielewicz, *Ann. Phys.* **152**, 239 (1984).
 [16] H.M. Pastawski and G. Usaj, *Phys. Rev. B* **57**, 5017 (1998).
 [17] P. Facchi and S. Pascazio, *Phys. Rev. Lett.* **89**, 080401 (2002), and references therein.
 [18] E.H. Lieb, T. Schultz and D.C. Mattis, *Ann. Phys.* **16**, 407 (1961); E.P. Danieli, H.M. Pastawski and P.R. Levstein, *Chem. Phys. Lett.* **382**, 306 (2004).
 [19] A.K. Chattah *et al.*, *J. Chem. Phys.* **119**, 7943 (2003).
 [20] H.M. Pastawski, *Phys. Rev. B* **44**, 6329 (1991), see Eq. 3.7; *ibid* **46**, 4053 (1992), see Eq. 4.11.
 [21] Z.L. Mádi *et al.*, *Chem. Phys. Lett.* **268**, 300 (1997).
 [22] V. Frerichs and A. Schenzle, *Phys. Rev. A* **44**, 1962 (1991).
 [23] W. M. Itano *et al.*, *Phys. Rev. A* **41**, 2295 (1990).
 [24] G. Teklemariam *et al.*, *Phys. Rev. A* **67**, 062316 (2003). J. Dalibard, Y. Castin and K. Mølmer, *Phys. Rev. Lett.* **68**, 580 (1992).
 [25] E.P. Danieli, H.M. Pastawski and G.A. Álvarez, *Chem. Phys. Lett.* **402**, 88 (2005).
 [26] A fit of the swapping dynamics using $(=)^2$ as free parameter gives the dipolar $(=)^2 = 4$ as expected [19]. The constant value for was obtained from fitting of the experimental data in the swapping phase, where the MKBE expression is valid.